



ARCHIVES  
of  
FOUNDRY ENGINEERING

DOI: 10.2478/afe-2014-0040

Published quarterly as the organ of the Foundry Commission of the Polish Academy of Sciences



ISSN (2299-2944)

Volume 14

Issue 2/2014

73 – 78

# Effect of Microstructure on Mechanical Properties of BA1055 Bronze Castings

**J. Labanowski\*, T. Olkowski**

Department of Materials Science and Welding, Gdansk University of Technology,  
11/12 Narutowicza, 80-233 Gdansk, Poland

\*Corresponding author. E-mail address: jlabanow@pg.gda.pl

Received 31.03.2014; accepted in revised form 30.04.2014

## Abstract

The article presents research results performed on aluminum bronze CuAl10Fe5Ni5 (BA1055) castings used for marine propellers. Metallographic studies were made on light microscope and a scanning electron microscope to assess quantitatively and qualitatively the alloy microstructure. It has been shown that the shape, size and distribution of the iron-rich  $\kappa$ -phase precipitates in bronze microstructure significantly affect its mechanical properties. With an increase in the number of small  $\kappa$ -phase precipitates increases the tensile strength of castings, while the presence of large globular precipitates improves ductility. Fragmentation and shape of  $\kappa$ -phase precipitates depends on many factors, particularly on the chemical composition of the alloy, Fe/Ni ratio, cooling rate and casting technology.

**Keywords:** Mechanical properties, Metallography, Ship propeller castings, Aluminium bronze

## 1. Introduction

Mechanical properties of marine propellers casting made of copper alloys are formed by the selection of chemical composition of the alloy and the use of casting technology ensuring efficient refinement as well as deoxidation and the removal of non-metallic inclusions, gases and slag from molten metal. The evaluation of the mechanical properties is made on the basis of sections taken from a test ingot cast separately or cast together with propeller screw. So established properties give only an approximate knowledge about the actual properties of the propeller casting that has different cooling conditions in sections thicker than test ingot, but they are reliable and accepted by the Marine Classification Societies.

Maintaining the chemical composition of copper alloy in the range recommended by the standards does not guarantee the required mechanical properties. Even small differences in the chemical composition of individual heats may significantly affect the mechanical properties while maintaining the same casting

conditions. Copper alloys Cu3 category according to the Polish Register of Shipping (PRS) [1] have usually five components, so you need to know the interactions of components. In the literature [2,3], you can find information about the effects of the individual components (Al, Fe, Ni, Mn) on the mechanical properties of aluminum bronzes but there is no sufficient information on joint action of components. For this reason, statistical studies were undertaken to develop appropriate regression equations describing the mechanical properties of castings as a function chemical composition of a copper alloy Cu 3 category. The results of these tests are presented in ref. [4].

Changes in chemical composition of the alloy are generally associated with specific changes in the microstructure of castings. Therefore, qualitative and quantitative study of the microstructure were undertaken in order to explain the reason for the changes in mechanical properties of obtained castings. The microstructure of aluminum bronze Cu-Al-Fe-Ni consists of  $\alpha$  solid solution,  $\alpha+\gamma_2$  eutectoid and precipitations of iron rich  $\kappa$ -phase. Based on the review of the literature it is assumed that the mechanical

properties of Cu3 category screw propellers castings largely depend on the location, size and shape of the precipitates of intermetallic  $\kappa$ -phase.  $\kappa$  phase, which chemical composition consists of copper, aluminum, iron and nickel can occur in several forms in the alloy microstructure [3,5-10]. The precipitation process of  $\kappa$ - phase described in [ 7, 8 ] is as follows. The first precipitates of the rich in iron phase  $\kappa_I$  are formed in the liquid metal already in shape of large rosettes, Fig. 1. Next precipitates of  $\kappa_{II}$  phase are formed in  $\beta$ -phase. They are smaller than  $\kappa_I$  precipitates and are also shaped as rosettes. Further precipitates, this time of the nickel-rich  $\kappa_{III}$  phase arise in the  $\alpha$ -phase in the zone adjacent to the  $\alpha/\beta$  border. They are small and have a platelet shape. In the end precipitates of an iron-rich  $\kappa_{IV}$  phase are formed, it takes place in the middle of  $\alpha$  phase grains. These  $\kappa_{IV}$  precipitates are small and have a spherical shape. With a reduction of Fe/Ni ratio in chemical composition of the alloy  $\kappa$  phase precipitates become more lamellar. It is generally believed that the proportion of  $\kappa$ -phase in the microstructure of aluminum bronze castings depends on the ratio of iron and nickel in the alloy, and optimal mechanical properties in the casts are obtained with a ratio of Fe/Ni>1

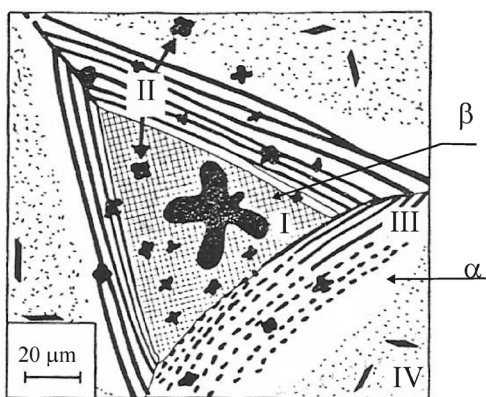


Fig. 1. Shapes of  $\kappa_I$ ,  $\kappa_{II}$ ,  $\kappa_{III}$ ,  $\kappa_{IV}$  phase precipitates in the BA1055 bronze microstructure [7]

## 2. Quantitative metallographic examinations

Examinations were performed on samples taken from separately cast ingots with a diameter of 60 mm of BA1055 bronze acc. to BS 1400:1985 (CuAl10Fe5Ni5) having a nominal chemical composition 8.8-10.0% Al, 4.0-5.5% Fe, 4.0 - 5.5% Ni  $Mn_{max}$  3.0%. Ten melts were selected with significantly different mechanical properties. Tensile strength ( $R_m$ ) was assumed as a basic characteristic property. Melts were chosen in the range of  $R_m$  647 - 693 MPa. The chemical compositions and mechanical properties of the castings are shown in Tables 1 and 2.

Metallographic examinations were performed on light microscopy Neophot-32. Determination of the percentage of alloy phases in the structure of the test samples was performed using the camera with adapter for metallographic quantitative analysis. Non-etched samples were used for assess percentage of  $\kappa$  phase,

because these precipitates were clearly visible and easily distinguishable from other structural components. Etched samples were used for determination  $\alpha$  phase and eutectoid  $\alpha+\gamma_2$ . Exemplary BA1055 bronze microstructures are shown in Figure 2 and 3. Graphical presentation of the relationship between tensile strength and the participation of phases in castings microstructure is shown in Figure 4 and 5.

Table 1.

Chemical compositions of examined BA1055 bronze casts, wt.%

| Heat | Al    | Fe    | Mn    | Ni    | Fe/Ni |
|------|-------|-------|-------|-------|-------|
| 847  | 9.540 | 4.090 | 1.074 | 4.210 | 0.971 |
| 849  | 9.659 | 4.301 | 1.136 | 4.403 | 0.977 |
| 858  | 9.824 | 4.032 | 1.276 | 4.081 | 0.988 |
| 859  | 9.860 | 4.052 | 1.353 | 4.124 | 0.983 |
| 861  | 9.750 | 4.190 | 1.366 | 4.309 | 0.972 |
| 914  | 9.606 | 4.054 | 1.028 | 4.156 | 0.975 |
| 916  | 9.644 | 4.100 | 1.071 | 4.180 | 0.981 |
| 917  | 9.790 | 4.210 | 1.120 | 4.260 | 0.988 |
| 919  | 9.713 | 4.090 | 1.252 | 4.224 | 0.968 |
| 920  | 9.801 | 4.118 | 1.114 | 4.197 | 0.981 |

Table 2.

Mechanical properties of examined BA1055 bronze casts

| Heat | $R_{p0.2}$<br>[MPa] | $R_m$<br>[MPa] | E<br>[%] | HB  | KV<br>[J] |
|------|---------------------|----------------|----------|-----|-----------|
| 847  | 279                 | 675            | 29.3     | 174 | 33        |
| 849  | 303                 | 667            | 23.7     | 179 | 26        |
| 858  | 304                 | 685            | 26.0     | 179 | -         |
| 859  | 304                 | 693            | 25.3     | 179 | 25        |
| 861  | 302                 | 671            | 21.5     | 179 | 24        |
| 914  | 284                 | 677            | 30.6     | 179 | -         |
| 916  | 291                 | 647            | 28.5     | 179 | 27        |
| 917  | 287                 | 664            | 19.9     | 179 | -         |
| 919  | 292                 | 683            | 27.6     | 179 | -         |
| 920  | 292                 | 666            | 21.5     | 179 | -         |

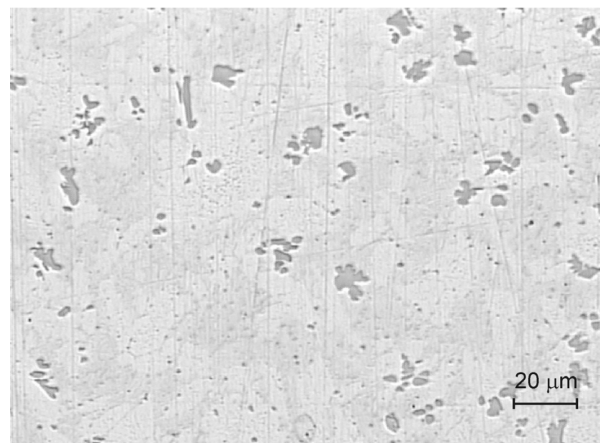


Fig. 2. BA1055 bronze microstructure. Non-etched sample. Visible precipitates of  $\kappa$ -phase

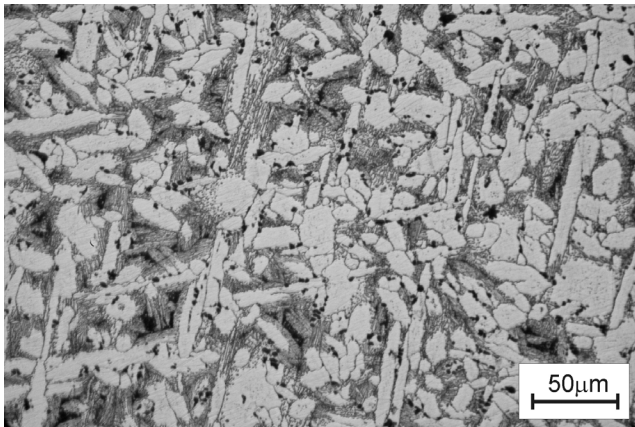


Fig. 3. Microstructure of cast BA1055 bronze; etch. Mi17Cu. The darker  $\kappa$ -phase precipitates at the matrix consisting of  $\alpha$ -phase (bright) and eutectoid  $\alpha+\gamma_2$  (grey)

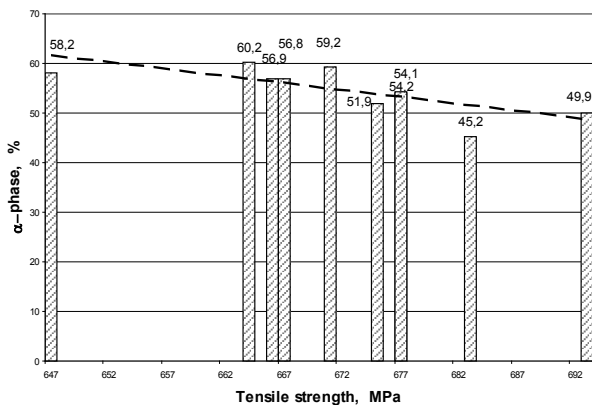


Fig. 4.  $\alpha$ -phase content in the microstructure of 10 selected BA1055 bronze castings of varying tensile strength; indicated a trend line

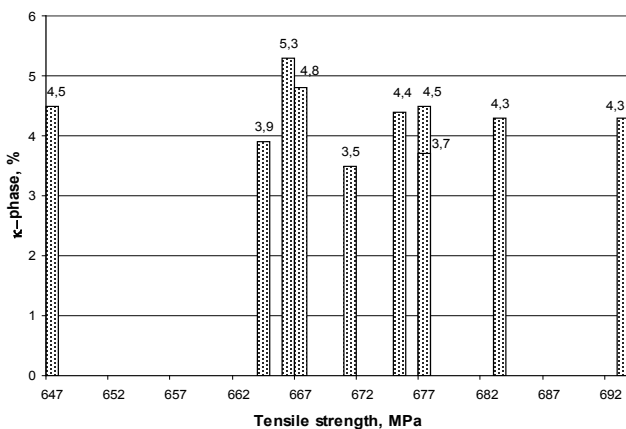


Fig. 5.  $\kappa$ -phase content in the microstructure of 10 selected BA1055 bronze castings of varying tensile strength

As it can be seen from Fig. 4, the strength of castings increases with decreasing content of  $\alpha$ -phase in the microstructure and increasing the eutectoid  $\alpha+\gamma_2$  share. There was no clear relationship between castings tensile strength and share of  $\kappa$ -phase in the structure (Fig. 5). Strengthening of BA1055 bronze castings may be related to the size and shape of  $\kappa$ -phase precipitates, which may be different [11].

In the studies of  $\kappa$ -phase precipitates size, image analysis were used, it allows to perform actual measurements of objects in the visual field. The study was performed on 10 fields for each sample. The mean effective surface and parameters characterizing the linear dimensions of the precipitates - Feret's diameter and the diameter of Martin were indicated. Figure 6 shows the average  $\kappa$ -phase precipitates area in the structure of ten BA1055 bronze melts of varying tensile strength. However direct relationship between these values was not found similar as it was in previously considered case of dependence of the total area of  $\kappa$ -phase precipitates in the structure of the tested heats.

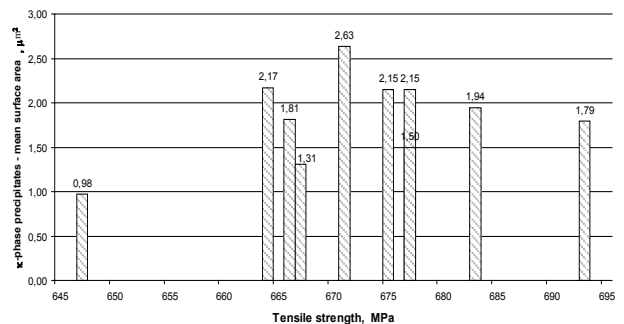


Fig. 6. Mean surface area of  $\kappa$ -phase precipitates in the microstructure of 10 selected BA1055 bronze castings of varying tensile strength

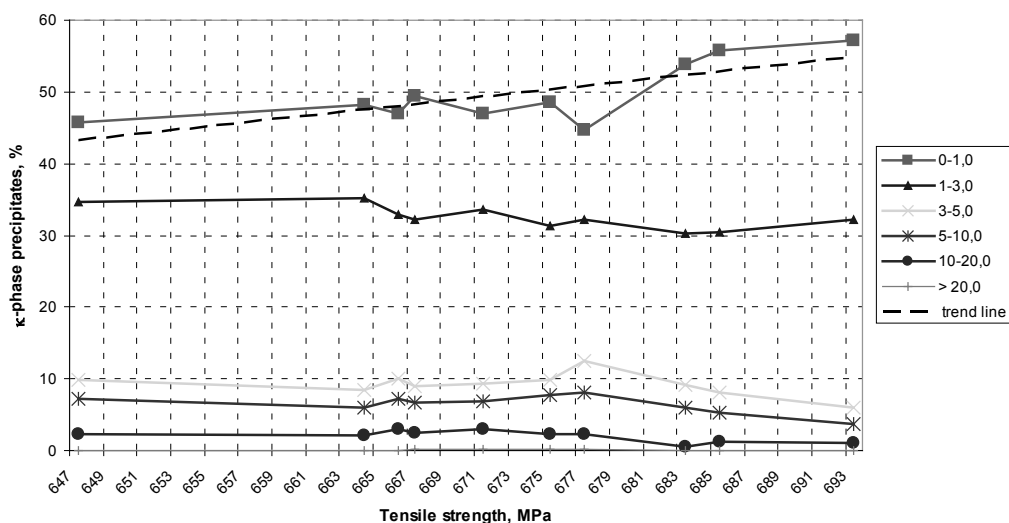
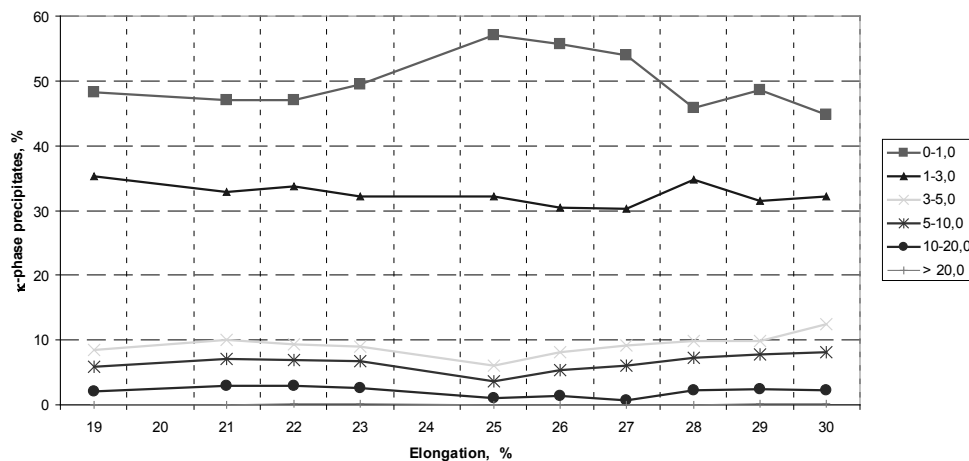
Therefore, studies were undertaken to determine the surface area of  $\kappa$ -phase precipitates distribution in the structure and show influence of particles of a certain size on the mechanical properties of the alloy. Analysis of the size distribution of  $\kappa$ -phase precipitates was performed in 10 places on each metallographic sample. The results are summarized in Table 3.

Studies have shown that approximately 50% of the  $\kappa$ -phase precipitates does not exceed surface area of  $1 \mu\text{m}^2$ , and therefore this group of precipitates has a decisive influence on the properties of the alloy. Confirmation of this observation is the increase in the strength properties of the examined melts BA1055 bronze progressing with the increase in the number of small  $\kappa$ -phase precipitates, Fig. 7. Effect of the  $\kappa$ -phase precipitates on the plasticity of examined melts is not clear. For melts exhibiting high plasticity, with elongation of more than 25%, there is a clear trend of increasing plasticity along with an increase of larger  $\kappa$ -phase particles share in the microstructure. For alloys with elongation below 23%, there was no significant influence of the  $\kappa$ -phase precipitates on the plasticity, Fig. 8.

Table 3.

Distribution of  $\kappa$ -phase precipitates of specified surface area in the BA1055 bronze microstructure

| Heat Sample | $R_m$ [MPa] | E [%] | Percentage share [%]      |                             |                             |                              |                               |                           |
|-------------|-------------|-------|---------------------------|-----------------------------|-----------------------------|------------------------------|-------------------------------|---------------------------|
|             |             |       | 0-1,0 [ $\mu\text{m}^2$ ] | 1,1-3,0 [ $\mu\text{m}^2$ ] | 3,1-5,0 [ $\mu\text{m}^2$ ] | 5,1-10,0 [ $\mu\text{m}^2$ ] | 10,1-20,0 [ $\mu\text{m}^2$ ] | >20,0 [ $\mu\text{m}^2$ ] |
| 917         | 664         | 19.9  | 48.26                     | 35.19                       | 8.51                        | 5.92                         | 2.12                          | 0.00                      |
| 920         | 666         | 21.5  | 46.95                     | 32.91                       | 10.01                       | 7.15                         | 2.91                          | 0.08                      |
| 861         | 671         | 21.5  | 47.01                     | 33.65                       | 9.30                        | 6.86                         | 2.96                          | 0.22                      |
| 849         | 667         | 23.7  | 49.49                     | 32.24                       | 8.91                        | 6.75                         | 2.52                          | 0.09                      |
| 859         | 693         | 25.3  | 57.12                     | 32.22                       | 5.97                        | 3.69                         | 1.00                          | 0.00                      |
| 858         | 685         | 26.0  | 54.75                     | 30.45                       | 8.13                        | 5.28                         | 1.30                          | 0.08                      |
| 919         | 683         | 27.6  | 53.93                     | 30.23                       | 9.23                        | 6.00                         | 0.61                          | 0.00                      |
| 916         | 647         | 28.5  | 45.76                     | 34.73                       | 9.90                        | 7.25                         | 2.27                          | 0.08                      |
| 847         | 675         | 29.3  | 48.52                     | 31.40                       | 9.84                        | 7.72                         | 2.35                          | 0.16                      |
| 914         | 677         | 30.6  | 44.70                     | 32.22                       | 12.53                       | 8.10                         | 2.26                          | 0.18                      |

Fig. 7. Tensile strength of ten BA1055 bronze melts depending on the size and distribution of  $\kappa$ -phase precipitatesFig. 8. Elongation of ten BA1055 bronze melts depending on the size and distribution of  $\kappa$ -phase precipitates

### 3. Microstructure examinations

Microstructure observations were performed using a scanning electron microscope Hitachi S-3400 with a 500-2000x magnification. Phase chemical composition examinations were performed using the X-ray microanalysis (EDS).

The study was performed on ten casts of BA1055 bronze. In order to reveal  $\kappa$ -phase precipitates samples were etched using reagent consisting: 5 g  $\text{FeCl}_3$ , 10 ml of HCl and 100 ml  $\text{H}_2\text{O}$ . The reagent used caused fast etching of  $\kappa$ -phase precipitates leaving pits, which clearly reflect the shape of the precipitates. For EDS analyzes non-etched samples were used, where  $\kappa$ -phase has not been degraded. Examples of the shape and position of the  $\kappa$ -phase precipitates in cast microstructure is shown in Figures 9, 10.

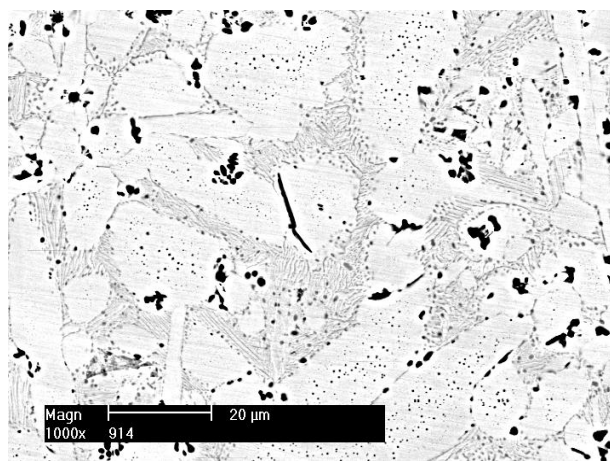


Fig. 9. The shape and location of the  $\kappa$ -phase precipitates in the microstructure of BA1055 bronze castings, (SEM)

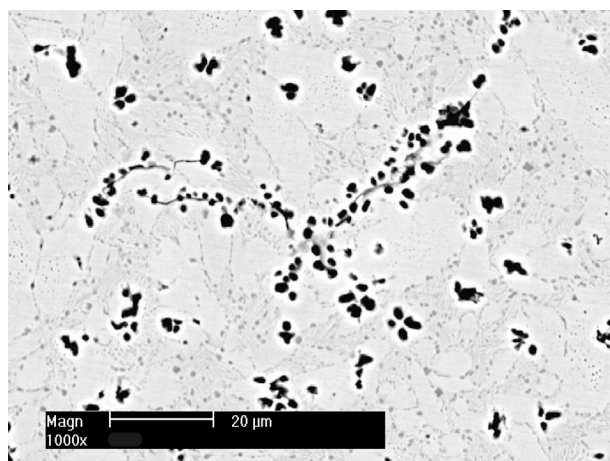
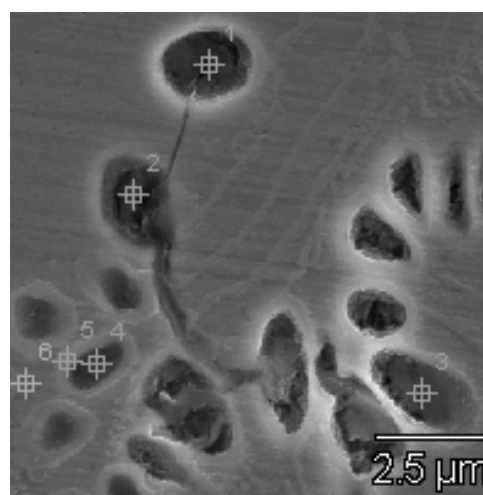


Fig. 10. The shape and location of the  $\kappa$ -phase precipitates in the microstructure of BA1055 bronze castings, (SEM)

The following  $\kappa$ -phase precipitates were observed in the microstructure of examined casts:

- large precipitates of  $\kappa_I$  and  $\kappa_{II}$  of rosette and spherical shape distributed mostly at the  $\alpha$ -eutectoid border, rarely inside areas of  $\alpha$ -phase and eutectoid,
- lamellar precipitates  $\kappa_{III}$  phase located at the  $\alpha$ -eutectoid border and inside eutectoid area,
- fine spherical precipitates  $\kappa_{IV}$  phase located inside  $\alpha$ -phase grains.

$\kappa$ -phase precipitates can occur at different stages of development measured by the size and chemical composition. Surprising was the finding of agglomerates of chain arranged globular particles of  $\kappa$ -phase linked with lamellar precipitates, Fig.10. This type of precipitates may cause a decrease in ductility of the alloy, but in tested melts this phenomenon was not observed, probably due to the small number of  $\kappa$ -phase agglomerates in the structure. Figure 11 indicates the places of the spot microanalysis of the chemical composition. Following analysis were performed: in points 1 to 4 - globular precipitates of  $\kappa$ -phase, in point 5 - narrow band around  $\kappa$ -phase precipitate and in point 6 - chemical composition of matrix ( $\alpha$  phase). The results of the analysis are given in the table under Fig. 11.

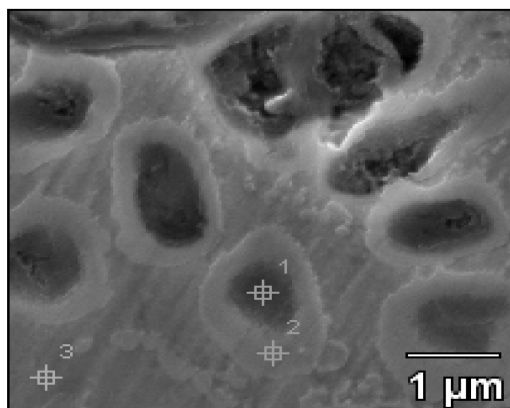


| Point | Al    | Mn   | Fe    | Ni    | Phase               |
|-------|-------|------|-------|-------|---------------------|
| pt1   | 4,35  | 2,27 | 33,69 | 23,22 | $\kappa$            |
| pt2   | 10,76 | 1,28 | 25,98 | 21,35 | $\kappa$            |
| pt3   | 5,07  | 2,41 | 51,82 | 20,67 | $\kappa$            |
| pt4   | 10,27 | 2,36 | 28,65 | 24,19 | $\kappa$            |
| pt5   | 14,81 | 1,94 | 6,19  | 10,31 | $\kappa$ - $\alpha$ |
| pt6   | 11,08 | 1,50 | 3,03  | 4,61  | $\alpha$            |

Fig. 11. Chemical composition in microareas of BA1055 bronze microstructure

Figure 12 shows a typical shell around the large spherical precipitates of  $\kappa$ -phase of different shade compared to the large surface of the  $\alpha$  grains. This is probably due to the different chemical composition in this micro area. Shell around lamellar precipitates of  $\kappa$ -phase are significantly smaller or do not exist at

all. The analysis of the chemical composition of the shell is shown in the table under Fig. 12.



| Point | Al    | Mn   | Fe    | Ni    | Phase               |
|-------|-------|------|-------|-------|---------------------|
| pt1   | 13,32 | 2,03 | 22,68 | 24,61 | $\kappa$            |
| pt2   | 19,27 | 1,63 | 10,08 | 13,26 | $\kappa$ - $\alpha$ |
| pt3   | 9,82  | 1,71 | 5,53  | 5,66  | $\alpha$            |

Fig. 12. Chemical composition in microareas of BA1055 bronze microstructure

Microanalysis of chemical composition revealed that the  $\alpha$  phase contains 8-9% Al, 2-5% Fe and 3-5% Ni. In the  $\alpha + \gamma_2$  eutectoid a higher content of aluminum 11-15% and nickel 6-10% was revealed. The chemical composition of the  $\kappa$ -phase varied within wide limits, particularly in terms of iron, the contents of which reached 52%, the nickel content remained constant at about 24%. Chemical composition analysis showed that the shell around  $\kappa$ -phase have less iron and nickel than precipitation, but more than at the  $\alpha$  phase, in which the precipitation occurred. Probably these are the areas of  $\kappa$ -phase under development where diffusion processes of Ni, Fe, Al and Cu between the matrix and precipitate take place.

## 4. Conclusions

1. It has been shown that the shape, size and distribution of  $\kappa$ -phase precipitates in cast bronze BA1055 microstructure significantly affect its mechanical properties.
2. With an increase in the number of small  $\kappa$ -phase precipitates, with an area smaller than  $1.0 \mu\text{m}^2$ , increases the tensile strength of castings, while the presence of large globular

precipitates of  $\kappa$ -phase improves plasticity. Lamellar precipitates decrease plastic properties of the alloy.

3. The chemical composition of the  $\kappa$ -phase varied within wide limits, particularly in terms of iron, the contents of which reached 52%, the nickel content remained constant at about 24%.

## References

- [1] Polish Register of Shipping. (2008). Classification Rules. Vol. 7, Part XIII Materials. Gdansk.
- [2] Piaseczny L. & Rogowski K. (2006) Modeling of mechanical properties from blade section thickness of the ship propeller sand casting. Conference Marine Transport. University of Catalonia. Barcelona, pp. 515-520.
- [3] Sokolov N.N., Lazarenko S.P. & Žuravlev V.I., (1971). Aluminium bronze propellers. Sudostroenie. Leningrad (in Russian).
- [4] Olkowski T. (2013). *Modelling of the mechanical properties of ship propeller castings made of copper alloy category Cu3*. Unpublished doctoral dissertation, Gdansk University of Technology, Poland (in Polish).
- [5] Kowarsch A. & Zaczek Z. (1989). *Cooper and its alloys in shipbuilding*. Publisher Marine, Gdańsk (in Polish).
- [6] Prowans S. & Wysiecki M. (1972). The effect of iron on the structure and phase transformations of aluminum bronzes. *Foundry Review*. 17(4), pp. 379-393 (in Polish).
- [7] Berezina P. (1973). Structure and mechanical properties of multi-component aluminum bronzes of the type CuAl10Fe5Ni5. *Gisereiforschung*, Jg.25, H.3, pp. 125-234.
- [8] Berezina P. (1973). Structure and mechanical properties of multi-component aluminum bronzes of the type CuAl10Fe5Ni5. *Giesereiforschung*, Jg.25, H.4, pp. 1-10.
- [9] Crofts W.J., Townsend D.W. & Bates A.P. (1964). Soundness and reproducibility of properties of sand-cast complex aluminium bronzes. *The British Foundryman*, 57 (2).
- [10] Stasiński A. & Grudowska A. (1971). Manganese bronze castings in the application of marine propellers. *Foundry Review*, 11, pp. 387-389 (in Polish).
- [11] Labanowski J. & Olkowski T. (2009). Effect of chemical composition and microstructure on mechanical properties of BA1055 bronze sand castings. *Advances in Materials Science*. Versita, Warsaw, 9(19), pp. 23-29.